Synthesis and Characterization of Thermo- and pH-Responsive Double-Hydrophilic Diblock Copolypeptides

Xiuqiang Zhang, Jingguo Li, Wen Li, and Afang Zhang*

School of Materials Science and Engineering, Zhengzhou University, Daxue Beilu 75, Zhengzhou 450052, China

Received June 30, 2007; Revised Manuscript Received August 24, 2007

Synthesis of novel double-hydrophilic diblock copolypeptides (BCPs), poly(L-glutamic acid)-*block*-poly(*N*-isopropylacrylamide) (**PLG$_n$PN$_m$**), and their thermoresponsive properties in aqueous solutions at different pH values are described. The diblock copolypeptides were synthesized by a combination of ring-opening polymerization (ROP) of γ-benzyl-L-glutamate *N*-carboxyanhydrides (**BLG-NCA**) and reversible addition−fragmentation chain transfer (RAFT) polymerization of *N*-isopropylacrylamide (*N*iPAM). A new class of RAFT agents (**CTA-2** and **CTA-3**) with amino-functional groups was designed for this purpose. Two different strategies, i.e., macrochain transfer agent (CTA) and macroinitiator routes, were utilized and compared on the control of the chemical structures of the resulting BCPs. Their block ratios and lengths are broadly varied (n = 21−600 and m =180−442). Their thermally switchable aggregation behaviors in aqueous solutions were investigated at the microscopic level by ^{1}H NMR spectroscopy and at the macroscopic level by turbidity measurements using UV/vis spectroscopy. The latter was also utilized for their lower critical aggregation temperature (LCAT) determination. The effects of block lengths and ratios as well as solution pH values on the collapse of *N*iPAM chain and aggregation process of BCPs were examined. This aggregation process was also followed by dynamic light scattering (DLS) measurements, and the thermally induced aggregate structures were investigated by transmission electron microscopy (TEM).

Introduction

Double-hydrophilic block copolymers (DHBCs) have recently become an interesting class of block copolymers (BCPs) because of their full water solubility, "smart" self-assembly behaviors, ability to interact with substrates, and potential as environmentally friendly and biocompatible substitutes to aggregates formed from organic solvents.[1] DHBCs of various compositions have been reported. Promising applications of DHBCs have covered areas such as drug and gene delivery,[2] catalysis,[3] surface modification,[4] as well as templating of inorganic nanocrystal formation.[5] DHBCs consist of all water-soluble blocks of different chemical nature. Normally, part block(s) just promote dissolution in aqueous solution, while the other(s) can form complexes with certain substances[6] or respond to external stimuli, such as pH values,[7] temperature,[8] ionic strength,[9] as well as light irradiation,[10] which then cause their chain conformation change and/or induce self-assembly. The solution behavior of DHBCs depends mainly on their chemical structures and is controlled through their stimuli-responsive characteristic(s). A specific case of stimuli-responsive DHBCs are those which contain a poly(*N*-isopropylacrylamide) [poly(*N*iPAM)] block.[11] Poly(*N*iPAM) has a lower critical solution temperature (LCST) in the range of approximately 32 °C with a sharp phase transition process,[12] which is especially attractive for bioapplications.[13]

Polypeptides conjugated with synthetic polymers have resulted in a promising class of BCPs, which have received much attention recently due to their tunable chemical structures and suprastructure formation[14] as well as attractive applications in different areas, such as tissue engineering and drug delivery,[15] biomimetic synthesis of ordered inorganic nanostructures,[16] etc. Polypeptides are especially of interest for self-assembly, and an even higher level of suprastructural controllability could be achieved when polypeptides are used as constituent blocks for BCPs since polypeptides can fold into well-ordered secondary structures like α helices or β sheets.[17] Block copolypeptides can be obtained normally via two routes: (a) ROP of NCAs initiated by an amino-terminated polymer chain or a transition-metal-based catalysis system (macroinitiator route) and (b) solid or solution-phase peptide synthesis and subsequent coupling with a carboxylated polymer or using the synthesized polypeptide as macro-CTA to mediate polymerization of a second monomer (macro-CTA route). Controlled radical polymerization techniques have been successfully applied for the synthesis of block copolypeptides, including peptide−polymer conjugates.[18]

To extend the idea to combine advantages from both DHBCs and copolypeptides in one matter[19] and afford copolymers with external stimuli-responsive properties at the same time, here we report on the novel stimuli-responsive diblock copolypeptides from poly(L-glutamic acid) and poly(*N*iPAM), whose water solubility is tunable by changing both the pH and temperature. Synthesis of BCPs was achieved through two strategies by combination of ROP of NCA and RAFT polymerization of *N*iPAM, differing in the starting block. The thermoresponsive properties and aggregation behaviors of BCPs with different block ratios and lengths in aqueous solutions of different pH values were investigated with ^{1}H NMR, UV/vis spectroscopy, and dynamic light scattering (DLS). The aggregate morphologies were investigated by TEM in some detail.

Experimental Section

Materials. 2-Dodecysulfanylthiocarbonylsulfanl-2-methyl propionic acid (**CTA-1**) was synthesized according to the literature method.[20]

* To whom correspondence should be addressed. Fax: +86-371-67766821. E-mail: azhang@zzu.edu.cn or zhang@mat.ethz.ch.

10.1021/bm700729t CCC: $37.00
Published on Web 10/05/2007

γ-Benzyl-L-glutamate *N*-carboxyanhydride (**BLG-NCA**) of high purity was synthesized by phosgenation of γ-benzyl-L-glutamate with triphosgene from anhydrous ethyl acetate (instead of THF), recrystallized twice by referring to the literature method,[21] and used immediately afterward. *N*iPAM was purified by recrystallization from a mixture of benzene and hexane (3/7, v/v). Azobis(isobutyronitrile) (AIBN) was recrystallized twice from methanol. Pure water was redistilled. Triethylamine (TEA) was dried over NaOH pellets. THF and dioxane (DOX) were dried by refluxing over sodium. Dichloromethane (DCM) and ethyl acetate were dried over CaH_2. Other reagents and solvents were purchased and used as received unless otherwise stated.

Instrumentation and Measurements. ^{1}H and ^{13}C NMR spectra were recorded on a Bruker 400 MHz spectrometer. The temperature-dependent ^{1}H NMR measurements were performed after the sample tube was kept at each preset temperature around 10 min for equilibrium. Mass spectrometry was carried out on a Waters a-Tof microspectrometer with an electrospray ionization source. Elemental analysis was performed on a Carlo Erba 1106 analyzer. Gel permeation chromatography (GPC) measurements were carried out at 40 °C using a PL-GPC 50 instrument equipped with two PLgel 5 μm MIXED-C columns (300 × 7.5 mm) and a differential refractive index detector. The system was operated with DMF (containing 1 g/L LiBr) as the eluent at a flow rate of 1 mL/min and calibrated with polymethyl methacrylate standards in the molar mass range from $M_p = 2.93 \times 10^3$ to 7.50×10^6 Da (Polymer Laboratories Ltd., U.K.). Column chromatography was performed using silica gel of 300−400 mesh. UV/vis turbidity measurements were carried out for lower critical aggregation temperature (LCAT) determination on a Varian Cary 1E (Australia) UV/vis spectrophotometer equipped with a thermostatically regulated bath. A solution of the respective diblock copolymer (6−7 mg) in pure water (4 mL) was added into a cell (path length 1 cm) which was placed in the spectrophotometer and heated at a rate of 1 °C·min^{-1}. The measurement at each temperature was done after the solution was kept at the preset temperature around 10 min for equilibrium. The temperature of the phase transition was considered the one at which the transmittance at $\lambda = 500$ nm had reached 50% of the value difference between the initial and final stages. DLS measurements were performed with a High Performance Zetasizer Nano instrument (Malvern, U.K.) using a light scattering apparatus equipped with a He−Ne (633 nm) laser and a thermoelectric Peltier temperature controller. The measurements were made at a scattering angle of $\theta = 173°$ ("backscattering detection"). The autocorrelation functions were analyzed with the CONTIN method. BCP solutions (1.5 mg·mL^{-1}) were filtrated through a 0.45 μm filter prior to use. Temperature-dependent DLS experiments were equilibrated 10 min at each step. Transmission electron microscopy (TEM) measurements were carried out on a FEI Tecnai G^2 20 instrument operated in the zero-loss bright-field mode and an acceleration voltage of 200 kV. Digital images were recorded with Gatan 794 CCD camera systems. The samples were prepared by placing a drop of an aqueous solution of the respective diblock copolymer at 20 or 50 °C onto a carbon-coated copper grid. The grid as well as all equipment used for the preparation were kept at either of these temperatures prior to use. The preparations were completed in less than 1 min for the sample preparation at 50 °C, which ensured a high reproducibility of the measurements. All samples were measured without staining.

CTA-Su. Compound **CTA-1** (1.00 g, 2.75 mmol) and *N*-hydroxysuccinimide (0.38 g, 3.3 mmol) were dissolved in dry DCM (100 mL), and then DCC (0.71 g, 3.40 mmol) was added at −15 °C. The mixture was stirred to room temperature for 12 h. The precipitate was removed by filtration. Chromatographic separation [silica gel, petrol ether/ethyl acetate (5:1, v/v)] gave the product as a yellow crystal (1.20 g, 95%). ^{1}H NMR (400 MHz, $CDCl_3$): $\delta = 0.88$ (t, 3 H, CH_3), 1.24 (t, 16 H, CH_2), 1.39 (t, 2 H, CH_2), 1.68 (t, 2H, CH_2), 1.83 (s, 6 H, CH_3), 2.80 (s, 4 H, CH_2), 3.31 (t, 2 H, CH_2). ^{13}C NMR (100 MHz, $CDCl_3$): $\delta =$ 14.16, 22.61, 25.40, 27.72, 28.31, 28.90, 29.01, 29.26, 29.36, 29.46, 29.54, 31.83, 37.02, 55.65, 179.12, 220.73. MS (ESI): *m*/*z* 484.2 (M + Na$^+$). Anal. Calcd for $C_{21}H_{35}NO_4S_3$ (461.2): C, 54.63; H, 7.64; N, 3.03. Found: C, 54.52; H, 7.70; N, 3.12.

CTA-2. A solution of *N*-Boc-ethylenediamine (0.65 g, 3.74 mmol) and TEA (0.45 g, 4.14 mmol) in DCM (20 mL) were dropped slowly into a solution of **CTA-Su** (2.60 g, 5.61 mmol) in DCM (30 mL) at −10 °C. The mixture was stirred for 12 h. The solution was washed with aqueous $NaHCO_3$ solution and brine and then dried over magnesium sulfate. Chromatographic separation [silica gel, petrol ether/ethyl acetate (5:1, v/v)] yielded **CTA-2** as yellow oil (1.70 g, 90%). ^{1}H NMR (400 MHz, $CDCl_3$): $\delta = 0.88$ (t, 3 H, CH_3), 1.25−1.67 (m, 20 H, CH_2), 1.43 (s, 9 H, CH_3), 1.72 (s, 6 H, CH_3), 3.23−3.34 (m, 6 H, CH_2), 4.80 (s, 1 H, NH), 6.89 (s, 1 H, NH). ^{13}C NMR (100 MHz, $CDCl_3$): $\delta =$ 14.06, 22.61, 25.70, 27.62, 28.31, 28.90, 29.01, 29.26, 29.36, 29.46, 29.54, 31.83, 37.02, 39.86, 40.98, 56.95, 79.38, 156.40, 173.02, 220.71. MS (ESI): *m*/*z* 529.3 (M + Na$^+$). Anal. Calcd for $C_{24}H_{46}N_2O_5S_3$ (506.3): C, 56.87; H, 9.15; N, 5.53. Found: C, 56.94; H, 9.08; N, 5.55.

CTA-3. Compound **CTA-2** (0.30 g, 0.59 mmol) was dissolved in an excess of TFA (2 mL) at 0 °C. After stirring for 1 h, an excess amount of methanol was added, and the solvent was evaporated in vacuum. Chromatographic separation (silica gel, DCM) gave the product as a yellow solid (0.24 g, 80%). ^{1}H NMR (400 MHz, $CDCl_3$): δ 0.88 (t, 3 H, CH_3), 1.25−1.69 (m, 20 H, CH_2), 1.69 (s, 6 H, CH_3), 3.13 (s, 2 H, CH_2), 3.28 (t, 2 H, CH_2), 3.49 (s, 2 H, CH_2). ^{13}C NMR (100 MHz, $CDCl_3$): $\delta =$ 14.58, 23.14, 25.77, 28.08, 29.44, 29.57, 29.80, 29.92, 30.02, 30.08, 32.36, 37.74, 39.02, 40.49, 57.29, 175.75, 221.92. MS (ESI): *m*/*z* 429.2 (M + Na$^+$). Anal. Calcd for $C_{19}H_{38}N_2OS_3$·TFA (406.2·TFA): C, 48.44; H, 7.55; N, 5.38. Found: C, 48.49; H, 7.61; N, 5.43.

General Procedure for ROP of BLG-NCA (A). The macroinitiator or **CTA-3** was dissolved in dry DMF or dioxane (DOX) inside a Schlenk tube; after the solution was degassed by three freeze−evacuate−thaw cycles, the required amount of **BLG-NCA** was added; polymerization was carried out at room temperature under N_2 for 3 days. The polymer was precipitated in diethyl ether twice, and the precipitated polymer was dried in high vacuum at 50 °C for 24 h.

General Procedure of RAFT Polymerization (B). The required amounts of *N*iPAM, **CTA-2** (or macro-CTA), and AIBN were dissolved in DMF inside a Schlenk tube. After the mixture was degassed by three freeze−evacuate−thaw cycles, polymerization was carried out at 80 °C under N_2 for 6−24 h. After cooling to room temperature, DCM was added into the solution and the polymer was precipitated into diethyl ether twice. The precipitated polymers were dried in high vacuum at 50 °C for 24 h.

PBLG$_n$-CTA. According to general procedure A from compound **CTA-3** (19.72 mg, 0.038 mmol), TEA (4.00 mg, 0.04 mmol) and **BLG-NCA** (0.30 g, 1.14 mmol) were added. Precipitation in diethyl ether/acetic acid (200:1) twice yielded the peptide as a slightly yellow foam (0.19 g, 65%). ^{1}H NMR (400 MHz, $CDCl_3$): $\delta = 0.88$ (t, CH_3), 1.25 (m, CH_2), 1.66 (s, CH_3), 1.9−2.6 (br, CH_2 + CH), 3.92 (br, CH), 5.0 (br, CH_2), 7.25 (br, C_6H_5), 8.33 (br, NH). ^{13}C NMR (100 MHz, $CDCl_3$): $\delta =$ 14.15, 22.70, 25.60, 29.35, 29.64, 30.96, 31.92, 56.94, 66.17, 67.98, 128.15, 128.48, 136.00, 172.07, 175.47, 207.08.

PBLG$_n$PN$_m$-CTA. According to general procedure B from polymer **PBLG-CTA** (0.05 g, 0.01 mmol), AIBN (0.54 mg, 0.0033 mmol) and *N*iPAM (0.34 g, 3 mmol) were added. Precipitation in diethyl ether twice yielded the block copolymer as a slight yellow powder (0.23 g, 53%). ^{1}H NMR (400 MHz, $CDCl_3$): $\delta = 0.88$ (t, CH_3), 1.14 (br, CH_3), 1.2−2.5 (br, CH_2 + CH), 3.99 (br, CH), 5.04 (br, CH_2), 6.47 [br, NH), 7.25 (br, C_6H_5), 8.33 (br, NH). ^{13}C NMR (100 MHz, $CDCl_3$): $\delta =$ 14.14, 22.62, 25.58, 30.84, 31.45, 34.40, 36.51, 41.30, 42.45, 56.85, 66.16, 128.14, 128.48, 136.00, 172.08, 174.29.

PN$_m$-CTA. According to general procedure B from the RAFT agent **CTA-2** (44.50 mg, 0.088 mmol), *N*iPAM (1.50 g, 13.3 mmol) and AIBN (0.96 mg, 0.0059 mmol) were added. Precipitation in diethyl ether (200 mL) twice gave the polymer as a yellow solid (1.20 g, 80%). ^{1}H NMR (400 MHz, $CDCl_3$): $\delta = 0.86$ (t, CH_3), 1.13 (br, CH_3), 1.24

Table 1. Conditions for and Results from ROP of **BLG-NCA** Initiated with **CTA-3** at Room Temperature in DMF

	polymerization conditions			GPC results[b]			
entries	[NCA]:[I][a]	time (h)	yield (%)	$M_n \times 10^{-4}$	PDI	DP_{GPC}	DP_{calcd}[c]
$PBLG_{24}$-CTA	33	27	65	0.53	1.38	24	21
$PBLG_{30}$-CTA	40	44	72	0.66	1.66	30	29
$PBLG_{36}$-CTA	50	72	73	0.80	1.29	36	36
$PBLG_{56}$-CTA	71	72	77	1.24	1.35	56	55
$PBLG_{79}$-CTA	110	107	72	1.74	1.30	79	79

[a] [NCA]:[I] = [**BLG-NCA**]:[**CTA-3**]. [b] DMF as eluent at 40 °C. [c] DP_{calcd} was calculated by yield × ([NCA]:[I]).

Table 2. Conditions for and Results from RAFT Polymerization of *N*iPAM at 70 °C in DOX with **PBLG-CTA** as Mediator

	polymerization conditions[a]			GPC results[c]		block length	
entries	[A]:[R]:[M][b]	time (h)	yield (%)	$M_n \times 10^{-4}$	PDI	ratio, r[d]	DP_{PN}[e]
$PBLG_{24}PN_{307}$-CTA	0.33:1:300	23	60	1.79	1.40	12.8	307
$PBLG_{24}PN_{353}$-CTA	0.33:1:350	29	50	3.31	1.50	14.7	353
$PBLG_{56}PN_{437}$-CTA	0.40:1:370	11	83	2.40	1.65	7.8	437
$PBLG_{56}PN_{179}$-CTA	0.30:1:490	24	47	3.10	1.60	3.2	179
$PBLG_{79}PN_{442}$-CTA	0.40:1:416	15	60	2.01	1.64	5.6	442

[a] **$PBLG_{24}$-CTA**, **$PBLG_{56}$-CTA**, and **$PBLG_{79}$-CTA** from Table 1 were used as the macro-CTA. [b] [A]:[R]:[M] = [AIBN]:[**PBLG-CTA**]:[*N*iPAM]. [c] DMF as eluent at 40 °C. [d] r = (DP of **PN**):(DP of PBLG). [e] DP_{PN} represents the polymerization degree of **PN** block, which was calculated according to r × (DP of PBLG).

Table 3. Conditions for and Results from RAFT Polymerization of *N*iPAM at 80 °C in DMF with **CTA-2** as Mediator

	polymerization conditions			GPC results[c]			
entries	[A]:[C]:[N][a]	time (h)	yield (%)	$M_n \times 10^{-4}$	PDI	DP	DP_{calcd}[d]
PN_{228}-CTA	0.10:1:250	19	91	2.34	1.23	207	228
PN_{270}-CTA	0.20:1:300	16	90	3.17	1.30	280	270
PN_{314}-CTA	0.07:1:330	36	95	3.23	1.16	285	314
PN_{346}-CTA	0.50:1:380[b]	30	91	3.37	1.27	298	346
PN_{360}-CTA	0.25:1:380[b]	35	95	3.56	1.24	314	360

[a] [A]:[C]:[N] = [AIBN]:[**CTA-2**]:[NiPAM]. [b] Polymerization at 90 °C. [c] DMF as eluent at 40 °C. [d] Calculated by yield × ([NiPAM]:[**CTA-2**]).

(br, CH_2), 1.31 (br, CH_2 + CH), 1.43 (s, CH_3), 1.61 (br, CH_2), 1.84 (br, CH_2), 2.04−2.30 (br, CH), 3.62 (br, CH_2), 3.73 (m, CH_2), 3.99 (br, CH), 6.15 (br, NH). ^{13}C NMR (100 MHz, $CDCl_3$): δ = 14.14, 22.63, 29.70, 36.38, 41.30, 42.53, 174.11.

PN_m(Boc). Polymer **PN_m-CTA** (1.00 g, 0.074 mmol) and AIBN (0.25 g, 1.52 mmol) were dissolved in dioxane (5 mL). After the solution was degassed by three freeze−evacuate−thaw cycles, the reaction was carried out at 80 °C under N_2 for 6 h. After cooling to room temperature, the solution was diluted with DCM (5 mL), precipitated into diethyl ether (200 mL) twice, and then dried in vacuum at 40 °C for 24 h, yielding the polymer as a white solid (0.95 g, 95%). ^{1}H NMR (400 MHz, $CDCl_3$): δ = 1.14 (br, CH_3), 1.27 (br, CH_3), 1.30−1.83 (br, CH_2 + CH_3), 1.44 (s, CH_3), 2.04−2.30 (br, CH), 3.73 (m, CH_2), 4.00 (br, CH), 6.28 (br, NH). ^{13}C NMR (100 MHz, $CDCl_3$): δ = 22.58, 29.70, 35.48, 41.33, 42.34, 162.59, 174.53.

PN_m(TFA). The polymer **PN_m(Boc)** (0.90 g, 0.066 mmol) was dissolved in trifluoroacetic acid (TFA, 4 mL) at 0 °C. After stirring for 2 h, an excess amount of methanol was added. The polymer was precipitated in diethyl ether twice and dried in vacuum at 40 °C for 24 h, yielding the polymer as a white solid (0.83 g, 92%). ^{1}H NMR (400 MHz, $CDCl_3$): δ = 1.14 (br, CH_3), 1.27 (br, CH_3), 1.43 − 1.80 (br, CH_2), 1.83 − 2.40 (br, CH), 3.50 (br, CH_2), 3.63 (br, CH_2), 4.00 (br, CH), 6.65 (br, NH). ^{13}C NMR (100 MHz, $CDCl_3$): δ = 22.57, 31.44, 35.90, 36.50, 41.30, 42.39, 162.59, 174.40.

PN_m-NH_2. KOH in MeOH solution (1 mol/L) was dropped at room temperature into the solution of **PN_m(TFA)** (0.80 g, 0.058 mmol) in MeOH (4 mL) to adjust the pH to 11−12. After stirring for 1 h, the polymer was precipitated in diethyl ether twice and then purified by column chromatography with DCM/MeOH (3:1) as the eluent, yielding the polymer (0.73 g, 91%). ^{1}H NMR (400 MHz, D_2O): δ = 1.01 (br, CH_3), 1.28 (br, CH_3), 1.42−1.85 (br, CH_2), 1.81−2.42 (br, CH), 3.63 (br, CH_2), 4.00 (br, CH), 6.25 (br, NH). ^{13}C NMR (100 MHz, $CDCl_3$): δ = 21.75, 35.00, 42.31, 49.10, 115.36, 163.22, 175.40.

$PBLG_nPN_m$. According to general procedure A from the macroinitiator **PN_m-NH_2** (0.15 g, 0.011 mmol) and the required amounts of **BLG-NCA** (according to the targeted molar mass). Precipitation in diethyl ether twice afforded the copolymers (see Table 4 for details). ^{1}H NMR (400 MHz, D_2O): δ = 1.14 (br, CH_3), 1.22 (br, CH_3), 1.33−1.80 (br, CH_3 + CH_2), 1.92−2.20 (br, CH + CH_2), 2.30−2.62 (br, CH_2), 3.65 (br, CH_2), 3.90 (br, CH), 4.00 (br, CH), 5.04 (br, CH_2), 6.60 (br, NH), 7.24 (br, benzyl). ^{13}C NMR (100 MHz, $CDCl_3$): δ = 22.50, 22.66, 25.75, 31.04, 41.38, 42.51, 66.00, 66.36, 68.11, 128.28, 128.64, 136.18, 172.25, 174.70, 175.66.

PLG_nPN_m. The copolymer **$PBLG_nPN_m$** (0.15 g) was dissolved in TFA (1 mL) at 0 °C, and then HBr/acetic acid (33%, 0.5 mL) was added. After stirring at room temperature for 2 h, an excess amount of diethyl ether was added to precipitate out the copolymer, and the precipitated polymer was washed with ethyl ether at least 4 times. After evaporation of solvents in vacuum, the residue was dried in vacuum at room temperature, yielding the copolymer as a red powder (0.13 g, 90%). ^{1}H NMR (400 MHz, D_2O): δ = 1.11 (br, CH_3), 1.30 − 1.80 (br, CH_2 + CH_3), 1.90−2.20 (br, CH_2 + CH), 3.65 (br, CH_2), 3.86 (br, CH), 4.28 (br, CH). ^{13}C NMR (100 MHz, D_2O): δ = 21.89, 28.33, 33.95, 42.04, 115.46, 117.78, 128.46, 129.10, 163.02, 163.30, 173.72, 181.74.

Self-Assembly. The respective diblock copolymer was dissolved in aqueous solutions with a concentration of 0.25 mg·mL^{-1} at pH = 8, 9, or 10 (adjusted carefully with concentrated NaOH aqueous solution), which was equilibrated for 1 day at room temperature in a closed vial under slow stirring and then put into an isothermal bath at 20 or 50 °C. The solutions became turbid within a few minutes at 50 °C and

Table 4. Conditions for and Results from ROP of **BLG-NCA** Initiated with $\mathbf{PN}_m\text{-}\mathbf{NH_2}$

	polymerization conditions[a]			GPC results[c]		block length		
entries	[I]:[M][b]	time (h)	yield (%)	$M_n \times 10^{-4}$	PDI	ratio, r[d]	DP_{PBLG}[e]	LCAT (°C)[f]
$\mathbf{PBLG_{27}PN_{228}}$	1:30	72	70	2.80	1.20	8.4	27	34.2
$\mathbf{PBLG_{57}PN_{228}}$	1:57	72	70	3.27	1.19	4.0	57	35.0
$\mathbf{PBLG_{79}PN_{228}}$	1:80	96	90	3.73	1.35	2.9	79	38.0
$\mathbf{PBLG_{114}PN_{228}}$	1:110	96	80	4.14	1.40	2.0	114	38.5
$\mathbf{PBLG_{86}PN_{360}}$	1:100	116	68	5.26	1.27	4.2	86	37.5
$\mathbf{PBLG_{180}PN_{360}}$	1:250	68	46	7.03	1.30	2.0	180	38.6
$\mathbf{PBLG_{600}PN_{360}}$	1:500	96	83	12.80	1.46	0.6	600	~41

[a] $\mathbf{PN_{228}\text{-}NH_2}$ and $\mathbf{PN_{360}\text{-}NH_2}$ were used as the macroinitiator. [b] [I]:[M] = [**PN**−$\mathbf{NH_2}$]:[**BLG-NCA**] [c] DMF as eluent at 40 °C. [d] r = (DP of **PN**):(DP of PBLG). [e] DP_{PBLG} represents the polymerization degree of PBLG block, calculated from DP_{PN}/r. [f] LCAT for the corresponding deprotected BCPs, $\mathbf{PLG}_n\mathbf{PN}_m$, at pH 10.0.

Scheme 1. Synthesis of RAFT Agents: **CTA-2** and **CTA-3**[a]

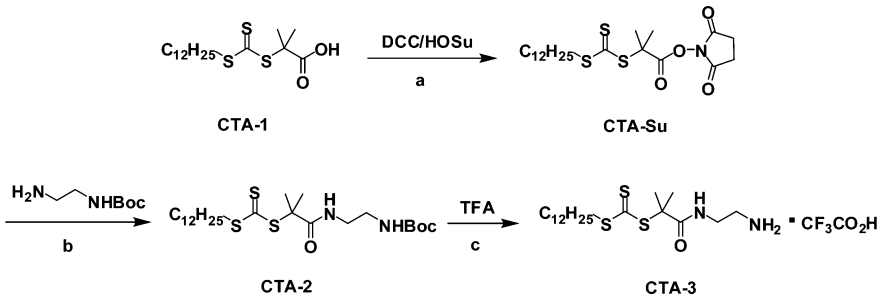

[a] Reagents and conditions: (a) DCC, HOSu, DCM, −15 °C, 12 h (95%); (b) *N*-Boc-ethylenediamine, TEA, −10 °C ,12 h (90%); (c) TFA, 0 °C,1 h (70%).

equilibrated for 15 h at the temperature before taking samples for the TEM measurements.

Results and Discussion

Synthesis of the Amino-Functionalized RAFT Agents. A new class of RAFT agents (**CTA-2** and **CTA-3**, see Scheme 1) with an amino-functional group in the leaving group was designed. These agents provide an easy way to combine ROP of α-amino acid NCA and RAFT polymerization of *N*iPAM for the synthesis of BCPs. Their synthesis started from the well-known carboxyl-terminated RAFT agent **CTA-1**. First, **CTA-1** was transformed into the active ester **CTA-Su** by the standard method,[22] which was then coupled with *N*-Boc-ethylene diamine at low temperature (−15 °C) in the presence of TEA and afforded **CTA-2** of high purity with excellent yield (95%). The low reaction temperature here is crucial as free amino group can attack the trithio group from the RAFT mediator efficiently even at room temperature[23] and leads to a wide mixture, which then takes much effort to purify. Finally, deprotection of the Boc group by TFA yielded the ammonium **CTA-3** as a yellow oil. This compound is quite stable at room temperature.

Synthesis of Block Copolypeptides. Synthesis of the block copolypeptides was tested with two different routes, i.e., macro-CTA and macroinitiator routes. The difference between these two routes relies on the starting block.

In the macro-CTA route, ROP of **BLG-NCA** first afforded the corresponding poly(γ-benzyl-L-glutamate) (PBLG) block with RAFT active end group, which was therefore used as the macro-CTA capable of letting another block grow off their active termini. The respective block copolypeptides were then synthesized by RAFT polymerization of *N*iPAM in the presence of the macro-CTA (Scheme 2). In order to synthesize the polypeptide block with a low polydispersity index (PDI), ROP of **BLG-NCA** with extremely pure dimethylformamide (DMF) as the solvent[24] was first initiated with the ammonium **CTA-3**

Scheme 2. Synthesis of the BCPs via Macro-CTA Route[a]

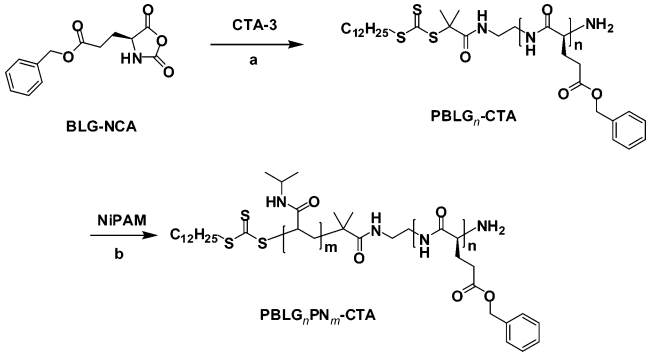

[a] Reagents and conditions: (a) **CTA-3**, TEA, DMF, room temperature, 72 h (65%); (b) AIBN, *N*iPAM, DMF, 80 °C, 12 h (53%).

according to Schlaad's method in order to avoid the activated monomer mechanism.[25] However, the polymerization yields were unfortunately low and normally below 5% (data are not shown). The reason for this is unclear.[26] Thus, addition of an equivalent amount of TEA transforms the ammonium **CTA-3** into its neutral state with free amine in the leaving group. This free amine showed much high reactivity in initiating the ROP of **BLG-NCA** and afforded $\mathbf{PBLG}_n\mathbf{\text{-}CTA}$ in acceptable yield (65−77%). Polymerization conditions and results are compiled in Table 1. The molar masses and PDIs of the polypeptide were determined by GPC in DMF. The polymerization degrees from GPC measurement (DP_{GPC}) are in good agreement with those from the calculated ones (DP_{calcd}), which suggest reasonable control in ROP of **BLG-NCA**. Although the polymerization went well, the PDIs of the polypeptides are slightly higher than expected and are normally in the range of 1.29−1.66. As proved by McCormick,[27] aminolysis of the trithiocarbonate group by the free amino end group from the polypeptide block should be the main side reaction here to cause the high PDI.

$\mathbf{PBLG}_n\mathbf{\text{-}CTA}$ was utilized as the macro-CTA for mediating the RAFT polymerization of *N*iPAM according to the well-

Scheme 3. Synthesis of the BCPs via Macroinitiator Route[a]

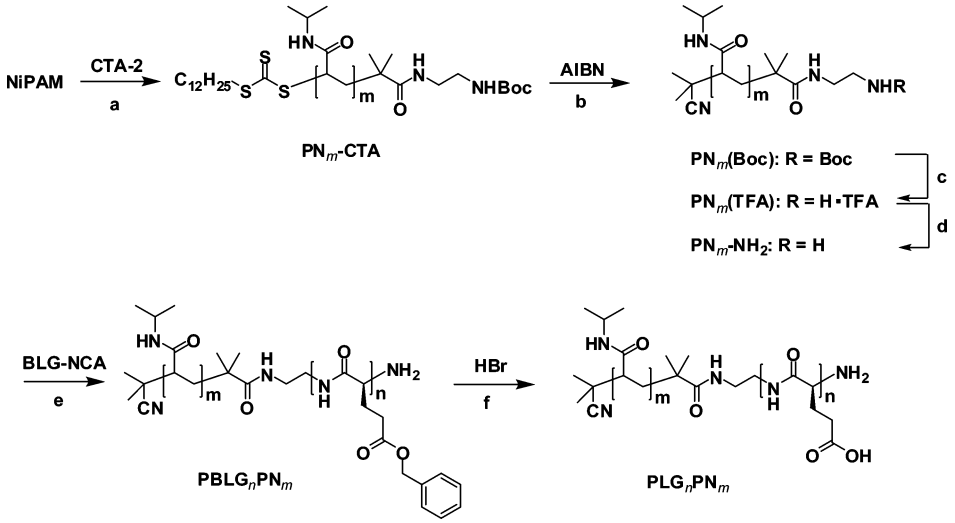

[a] Reagents and conditions: (a) **CTA-2**, AIBN, DMF, 80 °C, 12 h (95%); (b) AIBN, DOX, 80 °C, 10 h (90%); (c) TFA, 0 °C, 2 h (97%); (d) KOH·MeOH, MeOH, room temperature, 1 h (97%); (e) **BLG-NCA**, DMF, room temperature, 72 h (80%); (f) TFA, HBr/acetic acid, 1 h (90%).

known procedure from McCormick.[28] Two different solvents, DOX and DMF, were used for polymerization, respectively, and the former is better than the latter in achieving higher polymerization reactivity of *N*iPAM. Representative polymerization results from DOX are listed in Table 2. Block ratios (r) were determined by ^{1}H NMR spectroscopy. For this purpose the signal intensity of $-CH_2O$ from PBLG block at $\delta = 5.04$ was compared with that of $-CH$ from *N*iPAM block (**PN**) at $\delta = 3.99$. The block length ratios (r) were varied between $3.2 < r < 14.7$. GPC measurements obviously underestimated the molar masses of the block copolypeptides due to the difference of hydrodynamic volume of BCPs and linear polymethyl methacrylate standards, and therefore, the molar mass of **PN** block from GPC measurement (by subtracting that of the first one from the total BCP molar mass) is not reasonable (data are not shown). Instead, the polymerization degree of **PN** block, DP_{PN}, was obtained by calculating from the respective block length ratio (r) together with the DP of the first PBLG block. Nevertheless, the resulting diblock copolypeptides **PBLG$_n$PN$_m$-CTA** were not satisfactory in both the yield (47∼83%) and their PDI (1.40−1.65). The broadened PDI of the block copolypeptides may be caused by ill-defined end-group structures of the polypeptide block due to the aminolysis of RAFT end group and also the presence of some other side reactions in ROP of **BLG-NCA** itself.

For the macroinitiator route the synthesis started first from the RAFT polymerization of *N*iPAM in DMF by the known method[11j] and formed **PN** block with Boc-protected amino group at one of the chain ends. Detailed polymerization results are shown in Table 3. The polymerization degrees from GPC measurements are slightly different from those calculated from the yield and the original ratios of CTA to *N*iPAM. The difference of the molecular weight from GPC measurement and calculation is ascribed to the difference of the hydrodynamic volume of poly(*N*iPAM) and linear polymethyl methacrylate standards. Overall, PDIs of **PN$_m$-CTA** synthesized here are in the range of 1.16−1.30, which are acceptable for the RAFT polymerization method. Two different polymerization temperatures (80 and 90 °C) were applied, but PDIs of **PN$_m$-CTA** are in a similar range (compare entries **PN$_{228}$-CTA**, **PN$_{270}$-CTA**, and **PN$_{314}$-CTA** with **PN$_{346}$-CTA** and **PN$_{360}$-CTA** in Table 3). The polymerization degrees of **PN$_m$-CTA** were designed to be large enough and are in the range of 130−360 in order to afford the resulting BCPs with suitable thermoresponsiveness. In order to avoid some side reactions, such as aminolysis of the RAFT end group by the free amino group in the ROP process of NCA, which was encountered in the macro-CTA route, the RAFT end group from **PN$_m$-CTA** was first removed according to Perrier's method[29] with an excess amount of AIBN at 80 °C in DOX, therefore, yielding **PN$_m$(Boc)**. The protected amino group in **PN$_m$(Boc)** was then deprotected with excess TFA to afford the ammonium **PN$_m$(TFA)**, which was used as the macroinitiator for the ROP of **BLG-NCA** to form the block copolypeptides (Scheme 3). Similar to the situation in the macro-CTA route, here we also found that the initiation activity of the ammonium **PN$_m$(TFA)** for ROP of **BLG-NCA** is quite low. Therefore, **PN$_m$-(TFA)** was transformed into **PN$_m$-NH$_2$** by reaction with a slight excess of KOH in MeOH. As the purity of the macroinitiator is so crucial for synthesis of polypeptide of defined structures, **PN$_m$-NH$_2$** was purified carefully by column chromatography with DCM/MeOH (3:1, v/v) as eluent before polymerization. All chemical structures of corresponding homopolymers **PN$_m$-CTA**, **PN$_m$(Boc)**, and **PN$_m$(TFA)** were checked by ^{1}H NMR to verify completion of each reaction (see Figure 1a−c). Purified **PN$_m$-NH$_2$** has proved to be a suitable macroinitiator for synthesis of **PBLG$_n$PN$_m$**. Detailed polymerization conditions and a representative overview of the results are shown in Table 4. It can be seen that, except in the case of extremely long PBLG block case as for entry **PBLG$_{600}$PN$_{360}$**, PDIs of the block copolypeptides are among 1.19−1.40, which are in a reasonable range. By this route block copolypeptides **PBLG$_n$PN$_m$** with different block lengths ($n = 27-600$, $m = 228-360$) and block ratios ($r = 0.6-8.4$) were synthesized. Some of them have the same **PN** block length but varied PBLG block length in order to systematically investigate the effects of the chemical structures on their stimuli-responsive or self-assembly behaviors in aqueous solutions. Most BCPs gave monomodal GPC elution curves, except for some with extremely long PBLG block, such as for **PBLG$_{600}$PN$_{360}$**; there is a small shoulder in the low molar mass side in the GPC eluent curve. This shoulder should correspond to a small amount of homopolypetide. Figure 2 shows typical GPC elution curves to illustrate these. The block copolymer structures were also confirmed by comparison of the ^{1}H NMR spectrum of **PN$_{360}$(TFA)** (Figure 1c) with that of **PBLG$_{86}$PN$_{360}$** (Figure 1d). A full signal assignment is provided in the spectra.

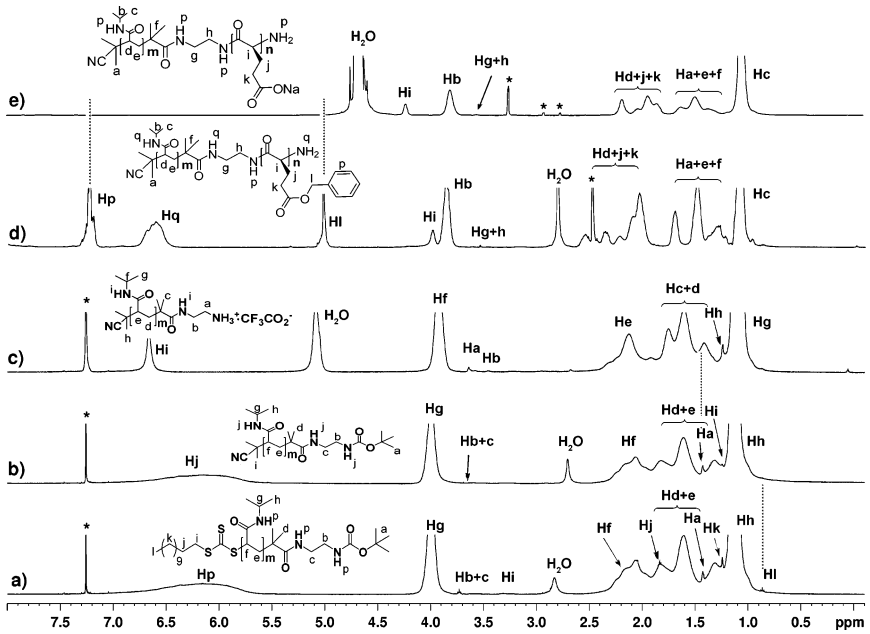

Figure 1. ^{1}H NMR spectra of (a) **PN_{360}-CTA** in $CDCl_3$, (b) **PN_{360}(Boc)** in $CDCl_3$, (c) **PN_{360}(TFA)** in $CDCl_3$ at 40 °C, (d) **$PBLG_{86}PN_{360}$** in d_6-DMSO at 100 °C, and (e) **$PLG_{86}PN_{360}$** in D_2O at pH 8.0. Solvent signals are marked with asterisks (*).

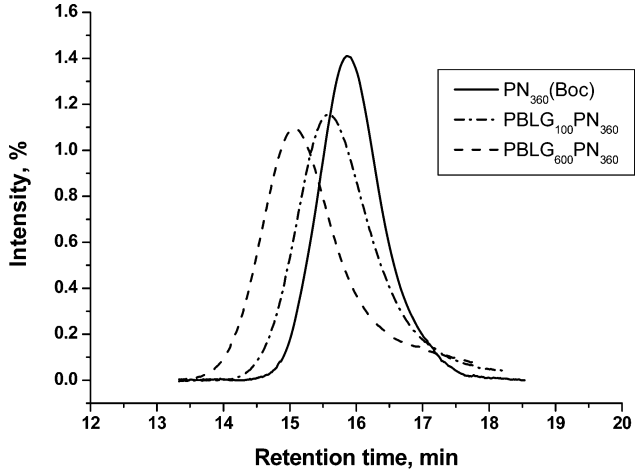

Figure 2. Typical GPC elution curves of **PN_{360}(Boc)**, **$PBLG_{86}PN_{360}$**, and **$PBLG_{600}PN_{360}$**.

The double hydrophilic copolymer **PLG_nPN_m** was achieved after quantitative removal of the benzyl group from the PBLG block in **$PBLG_nPN_m$** with HBr/glacial acetic acid by the standard method (step f in Scheme 3).[30] Figure 1d and e illustrates this point. The signals from the benzyl groups in **$PBLG_{86}PN_{360}$** at $\delta = 5.04$ and 7.24 (Figure 1d) disappeared completely upon deprotection (Figure 1e).

Stimuli-Responsive Aggregation Behavior of Block Copolypeptides by ^{1}H NMR Spectroscopy. BCPs with poly(*N*iPAM) block show similar thermoresponsive behaviors as the poly(*N*iPAM) homopolymers, but their LCATs are dependent on BCP's chemical structure, composition, or block ratios, etc. When a hydrophilic block is included, the LCATs of the corresponding BCPs increase. However, when a hydrophobic block is incorporated, the LCATs decrease.[31] The thermally induced aggregation behaviors of poly(*N*iPAM) homo- and block copolymers have been followed by ^{1}H NMR spectroscopy.[11a,j] The signal intensities in proton spectra from *N*iPAM chain showed a reversible decrease or increase when the aqueous solution temperature was shifted above or below their LCATs, which were interpreted in terms of a reversible collapse of the *N*iPAM chain followed by its aggregation. Therefore, the thermal aggregation behaviors of **PLG_nPN_m** were first investigated with ^{1}H NMR spectroscopy. This is to check how block lengths and ratios of the BCPs as well as aqueous solution pH values show effects on the collapse of *N*iPAM chain and their phase transition process. **PLG_nPN_m** becomes water soluble only when the aqueous solution pH is higher than 7.0, i.e., at neutral to basic conditions due to the carboxyl groups from **PLG** block. Thus, the hydrophilicity of **PLG_nPN_m** will increase with pH. Preliminary experiments proved that the proton NMR spectra of **$PLG_{600}PN_{360}$** in aqueous medium (pH 7.0) with a concentration of around 52 mg·mL^{-1} showed a reversible disappearance and reappearance of the *N*iPAM signals when the solution temperature changed between 25 and 50 °C. Therefore, further experiments were conducted to examine the detailed thermal aggregation behaviors at different solution pH values. Figure 3 shows representative temperature-dependent ^{1}H NMR spectra of **$PLG_{600}PN_{360}$** in aqueous solution at pH 7.0 in the temperature range from 27 to 50 °C. The signal intensities from **PLG** block remained as they were in the whole temperature range except for slight chemical shift changes, but the signal intensities from **PN** block (indicated by arrows) started to decrease obviously at around 29 °C, which is a clear indication that *N*iPAM chains start to collapse around this point. This temperature is close to that for the *N*iPAM homopolymers.[12a] These signal intensities continue decreasing upon increasing solution temperature and nearly disappeared completely above 40 °C. Similar temperature-dependent ^{1}H NMR measurements were also done when the solution pH values were adjusted by NaOH into 8.0 and 10.0, respectively, in order to check the effects of the solution pH on *N*iPAM chain collapse. Detailed ^{1}H NMR spectra are shown in the Supporting Information (Figures S1 and S2). To more accurately clarify the *N*iPAM chain collapse process, the ratios of proton signal intensity at $\delta = 3.98$ from **PN** block to that at $\delta = 2.52$ from PLG block were plotted against the solution temperature as shown in Figure 4. It can be seen from the curves that the signal intensities from **PN** block started to decrease (and the *N*iPAM chain started to collapse) at 28−29 °C, irrespective of the solution pH. The phenomenon, *N*iPAM chain collapse being independent to solution pH values, is not expected

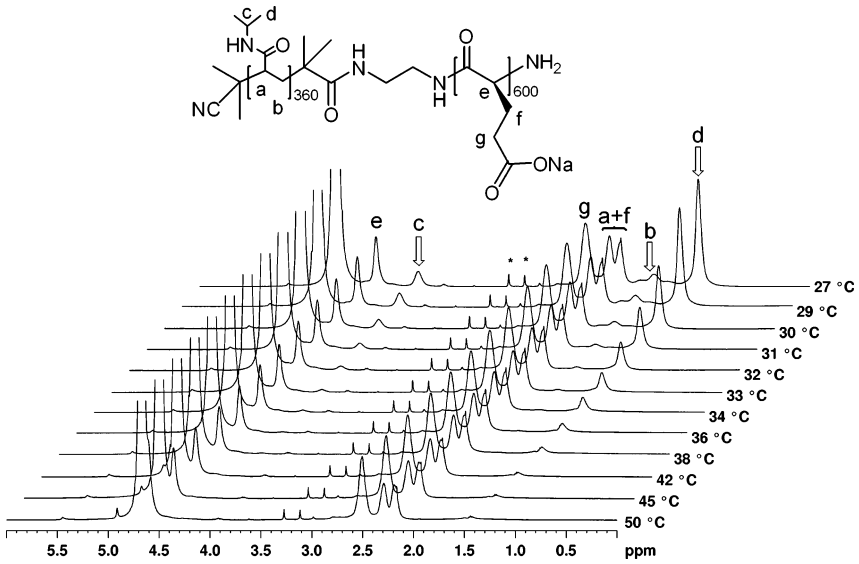

Figure 3. Temperature-dependent ^{1}H NMR spectra of **PBLG$_{600}$PN$_{360}$** in aqueous solution of pH 7.0 with a concentration of 52 mg·mL^{-1}. All spectra were oriented according to the same intensity of the peak (*g*) at $\delta = 2.52$. The three arrows indicate the poly(*N*iPAM) signals whose intensities decrease with increasing temperature. Solvent signals are marked with asterisks (*).

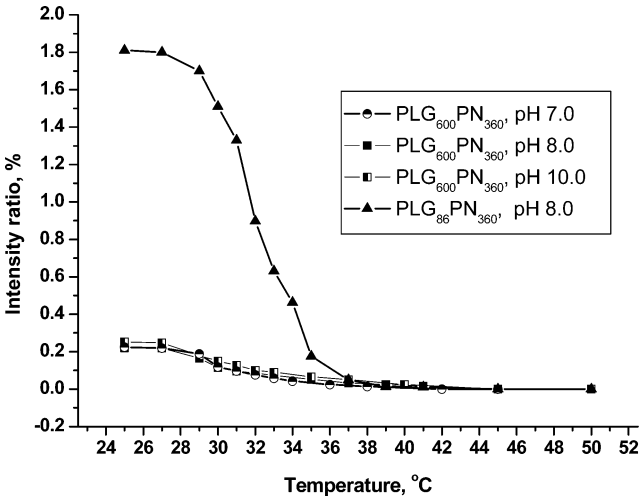

Figure 4. Plots of temperature vs the ratios of proton signal intensity at $\delta = 3.98$ from **PN** block to that at $\delta = 2.52$ from PLG block. Detailed temperature-dependent ^{1}H NMR spectra are shown in Figure 3 and in the Supporting Information (Figures S1−S3).

as the hydrophilicity of **PLG$_{600}$PN$_{360}$** should increase with solution pH, which then should lead to an increase of the LCAT of the BCPs. Furthermore, in all three pH cases the solutions in the NMR tube at 50 °C were completely clear by visual inspection, which suggests that although the NiPAM chain started to collapse from solution around 28 °C, no big and compact aggregates were formed that were able to scatter light at this stage. This is an indication that the low critical association process of the BCPs is somehow isolated from the collapse of *N*iPAM chain. Since poly(*N*iPAM) homopolymers with comparable chain length can form tight aggregates under these conditions,[32] here long PLG block obviously influences the BCPs' aggregation/solution behavior. This long PLG block seems to protect the collapsed *N*iPAM chain against tight aggregate formation. It is also necessary to point out here that the thermal transition process of **PLG$_{600}$PN$_{360}$** in any of the three pH value cases is very broad and covers a temperature range from 28 to 40 °C, which is also quite different from the sharp phase transition of poly(*N*iPAM) homopolymers.

In order to find out whether the length of PLG block plays a role on the phase transition process, BCP with a much shorter PLG block but the same length of **PN** block, **PLG$_{86}$PN$_{360}$**, was utilized for the temperature-dependent ^{1}H NMR measurements. The measurements were done with a solution pH of 8.0 and a concentration of 40 mg·mL^{-1} in the temperature range of 25−50 °C. Spectra are shown in the Supporting Information (Figure S3), and the proton signal intensity at $\delta = 3.98$ from *N*iPAM block starts to decrease at around 28 °C and disappears at about 40 °C (Figure 4). Therefore, the phase transition behavior of **PLG$_{86}$PN$_{360}$** is almost the same as in the case of **PLG$_{600}$PN$_{360}$**, which suggests that the block length of PLG does not contribute obviously to the collapse of *N*iPAM chain. However, in contrast, a solution of **PLG$_{86}$PN$_{360}$** in the NMR tube at 50 °C was turbid by visual inspection. This suggests that the *N*iPAM chain collapse in this case was followed by big or compact aggregate formation.

Turbidity Measurements Using UV/vis Spectroscopy for LCAT Determination. In order to understand the relationship between *N*iPAM collapse and chain aggregation in **PLG$_n$PN$_m$**, the aggregation behaviors of the BCPs were further investigated by turbidity measurements, aiming at their LCAT determination. Some of the LCATs are listed in Table 4. As expected, BCPs with relatively long **PN** block have a LCAT of 34.2 °C, which is very close to the poly(*N*iPAM) homopolymer. However, when extremely long **PLG** block was incorporated, the LCAT increased to around 41 °C in the case of **PLG$_{600}$PN$_{360}$**. **PLG$_n$PN$_m$** with the same **PN** block length ($m = 360$) but different **PLG** block length ($n = 86$ and 600, respectively) with the concentration of BCPs around 1.5−1.8 mg·mL^{-1} were used for the turbidity measurements, especially for investigating the effect of the block length.[33] Two different pH values (8.0 and 10.0) were also used in order to check the effect of solution pH values. The corresponding transmittance curves are shown in Figure 5. The transmittance curve of **PN** homopolymer (curve a) is also included for easy comparison. Comparing curves b and c from **PLG$_{86}$PN$_{360}$** with curve a from **PN$_{360}$-NH$_2$** one can easily see that the transition becomes much broader when PLG block is incorporated, which suggests a more complicated aggregation process is involved. The corresponding LCAT also increases from 33.5 °C for homopolymer **PN$_{360}$-NH$_2$** to 37.5 °C for **PLG$_{86}$PN$_{360}$**. Comparison of curve b from pH 8.0 with curve c from pH 10.0 leads to the conclusion that the solution pH has a very weak influence on the thermal transition process.

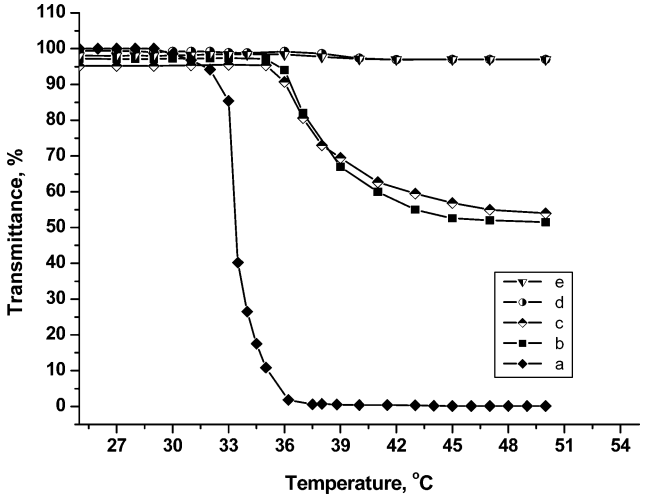

Figure 5. Transmittance vs temperature curves for aqueous solutions of (a) $\mathbf{PN_{360}}$-$\mathbf{NH_2}$, 1.5 mg·mL^{-1}, pH = 10.0, (b) $\mathbf{PLG_{86}PN_{360}}$, 1.5 mg·mL^{-1}, pH = 8.0, (c) $\mathbf{PLG_{86}PN_{360}}$, 1.5 mg·mL^{-1}, pH = 10.0, (d) $\mathbf{PLG_{600}PN_{360}}$, 1.8 mg·mL^{-1}, pH = 8.0, and (e) $\mathbf{PLG1_{600}PN_{360}}$, 1.8 mg·mL^{-1}, pH = 10.0.

Furthermore, the remaining transmittance at elevated temperature for an aqueous solution of $\mathbf{PLG_{86}PN_{360}}$ with a pH of 8.0 or 10.0 is around 55%. This suggests that although the solutions become turbid, the aggregates formed here are either not so big or not compact packed and thus are not able to scatter light efficiently. The LCAT for $\mathbf{PLG_{86}PN_{360}}$ is around 37.5 °C, which is much higher than that for *N*iPAM chain to collapse (according to the temperature-dependent ^{1}H NMR measurements, the latter started at around 28 °C). When an even longer **PLG** block was incorporated as in the case of $\mathbf{PLG_{600}PN_{360}}$, a very weak transition at even higher temperature range from 37 to 42 °C was observed (curves d and e in Figure 5). The transmittance is higher than 96% at elevated temperature; thus, the solution is still transparent up to 50 °C, irrespective of solution pH. This suggests that the long PLG block dominates the solution behavior of the corresponding BCP.

The difference between the LCAT from the turbidity measurements and the collapse temperature for *N*iPAM chain from temperature-dependent ^{1}H NMR measurements indicates aggregation of BCPs is not simultaneously followed by *N*iPAM chain collapse, at least in the cases investigated here.

DLS Measurements. The thermally induced aggregation behaviors of BCPs were also investigated by DLS study, and the results are shown in Figure 6A. Surprisingly, there are some aggregates at room temperature with a size in the range 90−160 nm, depending on the chemical composition and molar masses of the BCPs. As the solutions were optically clear at this stage, these aggregates must not be compact enough to scatter light. Poly(*N*iPAM) would not be able to form any aggregates from aqueous solution at temperature below its LCAT;[11j] therefore, these aggregates should be formed due to the interaction between the charged PLG blocks. When solution temperature increased to the corresponding LCAT, the aggregate size started to increase. For $\mathbf{PLG_{57}PN_{228}}$ and $\mathbf{PLG_{86}PN_{360}}$ (both BCPs have nearly the same block ratios but with different absolute block lengths) with solution pH value 8.0, an abrupt transition appeared at a temperature of approximately 34−35 °C. Above this temperature large aggregates with hydrodynamic diameters of around 360 and 220 nm were observed for $\mathbf{PLG_{57}PN_{228}}$ and $\mathbf{PLG_{86}PN_{360}}$, respectively. Thus, aggregates from $\mathbf{PLG_{57}PN_{228}}$ (with short chain lengths) are much bigger than those from $\mathbf{PLG_{86}PN_{360}}$ (with long block lengths). These

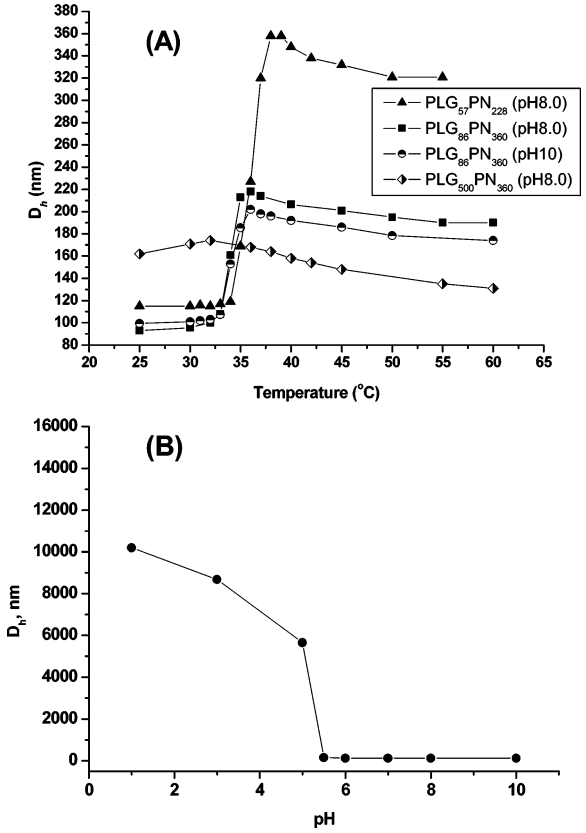

Figure 6. (A) Plots of the hydrodynamic diameter D_h as a function of temperature measured by DLS for aqueous solutions (1.5 mg·mL^{-1}) of $\mathbf{PLG_{57}PN_{228}}$ (pH 8.0), $\mathbf{PLG_{86}PN_{360}}$ (pH 8.0 and 10.0), and $\mathbf{PLG_{600}PN_{360}}$ (pH 8.0). (B) Plot of the hydrodynamic diameter D_h as a function of solution pH values measured by DLS for an aqueous solution (1.5 mg·mL^{-1}) of $\mathbf{PLG_{57}PN_{228}}$.

aggregates are comparable in size to what is usually observed for poly(*N*iPAM) homopolymers above their LCSTs[34] and are ascribed to aggregation of collapsed dehydrated poly(*N*iPAM) chains. Further increase of temperature caused shrinkage of the aggregates due to further dehydration of poly(*N*iPAM) chains. Comparing the results from pH 8.0 with those from pH 10.0 for $\mathbf{PLG_{86}PN_{360}}$ leads to the conclusion that solution pH has a very weak influence on the aggregate size. For BCPs with much longer PLG block, such as in the case of $\mathbf{PLG_{600}PN_{360}}$, the transition of aggregate size with temperature is not so pronounced, which suggests the long PLG block at basic condition dominates the BCP's solution behavior. The DLS results shown here are in good agreement with those from turbidity measurements, but the transient temperatures are slightly lower than these from turbidimetry. This phenomenon was also observed by Lutz in their different thermoresponsive polymer system.[35]

DLS measurements were also used to follow the pH-responsive behaviors of $\mathbf{PLG_{57}PN_{228}}$. Solution pH values were first adjusted with 10% NaOH solution into 10.0 and then carefully acidified with 10% HCl into different pH values from 8.0 to 1.0. The aggregate sizes were measured by DLS, and results are plotted in Figure 6B. With solution pH decreasing from 10 to 5.5, the aggregates had nearly the same size, which is around 120 nm. There is an abrupt transition appearing at a pH of approximately 5.5, and the solution became turbid by visual inspection. Below this pH very large aggregates with hydrodynamic diameters of a few micrometers were observed, and the aggregate size increases with the decrease of solution pH. At pH 1.0, aggregates with a size of around 10 μm formed. As the aggregates are quite big, they started to precipitate out

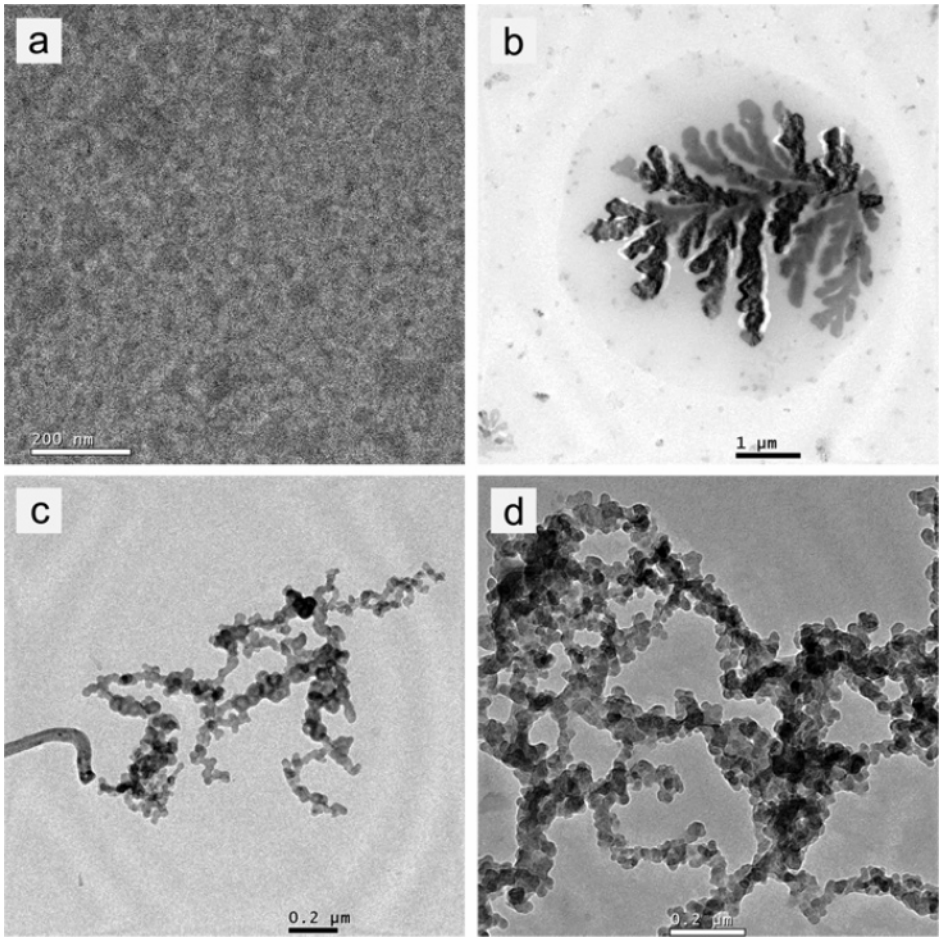

Figure 7. TEM images for $\mathbf{PLG_{57}PN_{228}}$ cast from an aqueous solution (0.25 mg·mL^{-1}): (a) pH 8.0, room temperature; (b) pH 8.0, 50 °C; (c) pH 9.0, 50 °C; (d) pH 10.0, 50 °C.

from the turbid solution. Although DLS measurement for such huge aggregates is not accurate anymore, the tendency should remain true. These results suggest that aggregates formed from BCPs are much larger in size by changing solution pH values than temperatures.

Thermally Induced Self-Assembly. On the basis of the evidence from ^{1}H NMR spectroscopy and the turbidity and DLS measurements, $\mathbf{PLG_nPN_m}$ undergo fully reversible aggregation above their LCATs. The morphologies of the aggregates formed therefore were further investigated by TEM measurements. $\mathbf{PLG_{57}PN_{228}}$ (with a long **PN** block but short PLG block) was selected for the assembly experiment, which has a LCAT of around 35 °C. TEM measurements were performed on the unstained samples from aqueous solution of different pH at room temperature and also at 50 °C. Although the morphologies of aggregates in solution could be quite different from their dry status, representative TEM images are shown in Figure 7. At room temperature, which is below the LCAT of $\mathbf{PLG_{57}PN_{228}}$, clear aqueous solution gave no visible aggregates (Figure 7a). While at 50 °C, which is above the LCST of $\mathbf{PLG_{57}PN_{228}}$, different kinds of aggregates formed from the turbid aqueous solution. At pH 8.0, up to 6−8 μm size of huge tree-like aggregates formed (Figure 7b). From the solution at pH around 9.0 aggregates with mixed morphologies, such as interconnected micelle-like aggregates with a size around 30−50 nm, together with some cylinder-shaped (or fiber-like) aggregates (with outer diameter around 20−50 nm) formed (Figure 7c). Only interconnected micelle-like aggregates were observed when solution pH became even higher, such as 10.0 (Figure 7d). It is clear that versatile assembled morphologies can be achieved from these dually stimuli-responsive BCPs by controlling both solution pH and temperature. Detailed investigations of the self-assembly behavior of $\mathbf{PLG_nPN_m}$ with different block lengths and ratios in aqueous solution are in process. Cryo-TEM measurements will be essential for this purpose.

Conclusions

Novel double-hydrophilic diblock copolypeptides poly(L-glutamic acid)-*block*-poly(*N*-isopropylacrylamide) ($\mathbf{PLG_nPN_m}$) with varied block ratios and lengths (r = 0.6−14.7, n = 21−600, m = 180−442) were synthesized by a particular combination of RAFT polymerization and ROP via macro-CTA and macroinitiator routes. These two routes were compared based on the controllability of the chemical structure of the resulting BCPs. Their molecular weight distributions are reasonably narrow (PDI = 1.19−1.40) when the macroinitiator route was applied.

The thermo-induced aggregation behaviors of $\mathbf{PLG_nPN_m}$ in aqueous solution at different pH values were investigated by temperature-dependent ^{1}H NMR spectroscopy, and their LCATs were determined by turbidity measurements. PLG block does not interfere obviously with the collapse of *N*iPAM chain at different solution pH, but it does shift the aggregation process of BCPs into higher temperature. From the big differences between the temperatures for *N*iPAM chain to collapse (28 °C) and those for BCP to aggregate (higher than 36 °C for $\mathbf{PLG_{86}PN_{360}}$ and 38 °C for $\mathbf{PLG_{600}PN_{360}}$), aggregation of BCPs does not instantaneously follow *N*iPAM chain collapse. DLS

measurements proved the thermally induced aggregation behaviors at different solution pH values. There are some aggregates with a size of 90−160 nm at room temperature. These aggregate sizes continue to grow upon heating above their LCATs and reached a maximum size of around 360 and 220 nm for $\mathbf{PLG_{57}PN_{228}}$ and $\mathbf{PLG_{86}PN_{360}}$, respectively, which then shrunk due to deeper dehydration upon further increase of the solution temperature. The pH-responsive (from pH 10.0 to 1.0) aggregation process of $\mathbf{PLG_{57}PN_{228}}$ was also followed with DLS measurements, and very similar aggregation behaviors but with much large aggregates were observed compared to the thermo-responsive ones. Solution pH values have a very weak influence on collapse of the *N*iPAM chain at basic conditions but strong effects on the self-assembled morphologies. Aggregates of different morphologies such as huge tree-like (size up to 6−8 μm), interconnected round-shaped (30−50 nm), and fiber-like (cylinder shaped) aggregates formed from dilute aqueous solution of the block copolypeptides with pH 8.0, 9.0, or 10.0 at 50 °C, respectively. Their dually responsive characteristics and versatile assembled morphology formation from aqueous solution make this kind of novel block copolypeptides interesting candidates for many aspects, such as in self-assembly, nanotemplating, and biomineralization.[36]

Acknowledgment. We thank Profs. Shijun Zheng, Mincan Wang, Tiesheng Li, and Haijun Zhang (Zhengzhou University) for their kind support with different measurements. Mr. Jiatao Yan and Dr. Jintao Wang are thanked for their help with some experiments. Ms. Suyang Zhang is thanked for her help with the manuscript. Support of the NMR measurements from the Analysis and Measurement Center of Zhengzhou University is appreciated. This work has been financially supported by the National Natural Science Foundation of China (grant nos. 20374047 and 20574062).

Supporting Information Available. Temperature-dependent ^{1}H NMR spectra (25−50 °C) in D_2O of $\mathbf{PLG_{86}PN_{360}}$ (pH 8.0) and $\mathbf{PLG_{600}PN_{360}}$ (pH 8.0 and 10.0). This material is available free of charge via the Internet at http://pubs.acs.org.

References and Notes

(1) (a) Cölfen, H. *Macromol. Rapid Commun.* **2001**, *22*, 219−252. (b) Butun, V.; Liu, S.; Weaver, J. V. M.; Bories-Azeau, X.; Cai, Y.; Armes, S. P. *React. Funct. Polym.* **2006**, *66*, 157−165.
(2) Kabanov, A. V.; Kabanov, V. A. *Adv. Drug Delivery Rev.* **1998**, *30*, 49−60.
(3) (a) Riley, T.; Stolnik, S.; Heald, C. R.; Xiong, C. D.; Garnett, M. C.; Illum, L.; Davis, S. S.; Purkiss, S. C.; Barlow, R. J.; Gellert, P. R. *Langmuir* **2001**, *17*, 3168−3174. (b) Semagina, N. V.; Bykov, A. V.; Sulman, E. M.; Matveeva, V. G.; Sidorov, S. N.; Dubrovina, L. V.; Valetsky, P. M.; Kiselyova, O. I.; Khokhlov, A. R.; Stein, B.; Bronstein, L. M. *J. Mol. Catal. A: Chem.* **2004**, *208*, 273−284.
(4) (a) Mahlting, B.; Gohy, J. F.; Jerome, R.; Stamm, M. *J. Polym. Sci., Part B: Polym. Phys.* **2001**, *39*, 709−718. (b) Webber, G. B.; Wanless, E. J.; Armes, S. P.; Tang, Y.; Li, Y.; Biggs, S. *Adv. Mater.* **2004**, *16*, 1794−1798.
(5) Yu, S. H.; Cölfen, H. *J. Mater. Chem.* **2004**, *14*, 2124−2147.
(6) (a) Laschewsky, A.; Mertoglu, M.; Kubowicz, S.; Thuenemann, A. F. *Macromolecules* **2006**, *39*, 9337−9345. (b) Xu, J.; Ge, Z.; Zhu, Z.; Luo, S.; Liu, H.; Liu, S. *Macromolecules* **2006**, *39*, 8178−8185.
(7) (a) Sfika, V.; Tsitsilianis, C.; Kiriy, A.; Gorodyska, G.; Stamm, M. *Macromolecules* **2004**, *37*, 9551−9560. (b) Vamvakaki, M.; Palioura, D.; Spyros, A.; Armes, S. P.; Anastasiadis, S. H. *Macromolecules* **2006**, *39*, 5106−5112.
(8) (a) Weissman, J. M.; Sunkara, H. B.; Tse, A. S.; Asher, S. A. *Science* **1996**, *274*, 959−963. (b) Hu, Z.; Chen, Y.; Wang, C.; Zheng, Y.; Li, Y. *Nature* **1998**, *393*, 149−152.
(9) Pispas, S. *J. Polym. Sci., Part A: Polym. Chem.* **2006**, *44*, 606−613.
(10) (a) Yu, S. H.; Cölfen, H.; Mastai, Y. *J. Nanosci. Nanotechnol.* **2004**, *4*, 291−298. (b) Athanassiou, A.; Kalyva, M.; Lakiotaki, K.; Georgiou, S.; Fotakis, C. *Adv. Mater.* **2005**, *17*, 988−992.
(11) (a) Arotcarena, M.; Heise, B.; Ishaya, S.; Laschewsky, A. *J. Am. Chem. Soc.* **2002**, *124*, 3787−3793. (b) Motokawa, R.; Morishita, K.; Koizumi, S.; Nakahira, T.; Annaka, M. *Macromolecules* **2005**, *38*, 5748−5760. (c) Han, D. H.; Pan, C. Y. *Macromol. Chem. Phys.* **2006**, *207*, 836−843. (d) Kulkarni, S.; Schilli, C.; Grin, B.; Müller, A. H. E.; Hoffman, A. S.; Stayton, P. S. *Biomacromolecules* **2006**, *7*, 2736−2741. (e) Zhang, W.; Jiang, X.; He, Z.; Xiong, D.; Zheng, P.; An, Y.; Shi, L. *Polymer* **2006**, *47*, 8203−8209. (f) Convertine, A. J.; Lokitz, B. S.; Vasileva, Y.; Myrick, L. J.; Scales, C. W.; Lowe, A. B.; McCormick, C. L. *Macromolecules* **2006**, *39*, 1724−1730. (g) Qin, S.; Geng, Y.; Discher, D. E.; Yang, S. *Adv. Mater.* **2006**, *18*, 2905−2909. (h) You, Y. Z.; Oupicky, D. *Biomacromolecules* **2007**, *8*, 98−105. (i) Skrabania, K.; Kristen, J.; Laschewsky, A.; Akdemir, O.; Hoth, A.; Lutz, J. F. *Langmuir* **2007**, *23*, 84−93. (j) Cheng, C.; Schmidt, M.; Zhang, A.; Schlüter, A. D. *Macromolecules* **2007**, *40*, 220−227.
(12) (a) Schild, H. G. *Prog. Polym. Sci*. **1992**, *17*, 163−249. (b) Ono, Y.; Shikata, T. *J. Am. Chem. Soc.* **2006**, *128*, 10030−10031.
(13) Chang, J. H.; Shim, C. H.; Kim, B. J.; Shin, Y.; Exarhos, G. J.; Kim, K. J. *Adv. Mater.* **2005**, *17*, 634−637.
(14) (a) Deming, T. J. *Adv. Polym. Sci.* **2006**, *202*, 1−18. (b) Löwik, D. W. P. M.; Ayres, L.; Smeenk, J. M.; Van Hest, J. C. M. *Adv. Polym. Sci.* **2006**, *202*, 19−52. (c) Schlaad, H. *Adv. Polym. Sci.* **2006**, *202*, 53−73. (d) Klok, H.-A.; Lecommandoux, S. *Adv. Polym. Sci.* **2006**, *202*, 75−111.
(15) (a) Duncan, R. *Nat. Rev. Drug. Disc.* **2003**, *2*, 347−360. (b) Osada, K.; Kataoka, K. *Adv. Polym. Sci.* **2006**, *202*, 53−74.
(16) (a) Cha, J. N.; Stucky, G. D.; Morse, D. E.; Deming, T. J. *Nature* **2000**, *403*, 289−292. (b) Euliss, L. E.; Grancharov, S. G.; O'Brien, S.; Deming, T. J.; Stucky, G. D.; Murray, C. B.; Held, G. A. *Nano Lett.* **2003**, *3*, 1489−1493.
(17) Voet, D.; Voet, J. G. *Biochemistry*, 2nd ed.; Wiley: New York, 1995; Chapter 32.
(18) (a) Becker, M. L.; Liu, J.; Wooley, K. L. *Chem. Commun.* **2003**, 180−181. (b) Mei, Y.; Beers, K. L.; Byrd, H. C. M.; VanderHart, D. L.; Washburn, N. R. *J. Am. Chem. Soc.* **2004**, *126*, 3472−3476. (c) Rettig, H.; Krause, E.; Börner, H. G. *Macromol. Rapid Commun.* **2004**, *25*, 1251−1256. (d) Brzezinska, K. R.; Deming, T. J. *Macromol. Biosci.* **2004**, *4*, 566−569. (e) Dong, C.-M.; Sun, X.-L.; Faucher, K. M.; Apkarian, R. P.; Chaikof, E. L. *Biomacromolecules* **2004**, *5*, 224−231. (f) Bontempo, D.; Maynard, H. D. *J. Am. Chem. Soc.* **2005**, *127*, 6508−6509. (g) ten Cate, M. G. J.; Rettig, H.; Bernhardt, K.; Börner, H. G. *Macromolecules* **2005**, *38*, 10643−10649. (h) Steig, S.; Cornelius, F.; Heise, A.; Knoop, R. J. I.; Habraken, G. J. M.; Koning, C. E.; Menzel, H. *Macromol. Symp.* **2007**, *248*, 199−206. (i) Boyer, C.; Bulmus, V.; Liu, J.; Davis, T. P.; Stenzel, M. H.; Barner-Kowollik, C. *J. Am. Chem. Soc.* **2007**, *129*, 7145−7154.
(19) Meyer M.; Schlaad H. *Macromolecules* **2006**, *39*, 3967−3970.
(20) Lai, J. T.; Filla, D.; Shea, R. *Macromolecules* **2002**, *35*, 6754−6756.
(21) (a) Blout, E. R.; Karlson, R, H. *J. Am. Chem. Soc.* **1956**, *78*, 941−947. (b) Daly, W. H.; Poche, D. *Tetrahedron Lett.* **1988**, *29*, 5859−5862.
(22) Hamphery, J. M.; Chamberlin, A. R. *Chem. Rev.* **1997**, *97*, 2243−2266.
(23) Mayadunne, R. T. A.; Rizzardo, E.; Chiefari, J.; Krstina, J.; Moad, G.; Postma, A.; Thang. S. H. *Macromolecules* **2000**, *33*, 243−245. (a) Lima, V.; Jiang, X.; Brokken-Zijp, J.; Schoenmakers, P. J.; Klumperman, B.; Van Der Linde, R. *J. Polym. Sci., Part A: Polym. Chem.* **2005**, *43*, 959−973. (b) Patton, D. L.; Mullings, M.; Fulghum, T.; Advincula, R. C. *Macromolecules* **2005**, *38*, 8597−8602. (c) Qiu, X.-P.; Winnik, F. M. *Macromol. Rapid Commun.* **2006**, *27*, 1648−1653. (d) Xu, J.; He, J.; Fan, D.; Wang, X.; Yang, Y. *Macromolecules* **2006**, *39*, 8616−8624. (e) Zhao, Y.; Perrier, S. *Macromolecules* **2006**, *39*, 8603−8608.
(24) Aliferis, T.; Iatrou, H.; Hadjichristidis, N. *Biomacromolecules* **2004**, *5*, 1653−1656.
(25) Dimitrov, I.; Schlaad, H. *Chem. Commun.* **2003**, 2944−2945.
(26) Lutz, J.-F.; Schütt, D.; Kubowicz, S. *Macromol. Rapid Commun.* **2005**, *26*, 23−28.
(27) McCormick, C. L.; Lowe, A. B. *Acc. Chem. Res.* **2004**, *37*, 312−325.
(28) Convertine, A. J.; Ayres, N.; Scales, C. W.; Lowe, A. B.; McCormick, C. L. *Biomacromolecules* **2004**, *5*, 1177−1180.

(29) Perrier, S.; Takolpuckdee, P.; Mars, C. A. *Macromolecules* **2005**, *38*, 2033−2036.
(30) (a) Ben-Ishai, D.; Berger, A. *J. Org. Chem.* **1952**, *17*, 1564−1570. (b) Blout, E. R.; Idelson, M. *J. Am. Chem. Soc.* **1956**, *78*, 497−498. (c) Wang, Y.; Chang. Y. C. *Macromolecules* **2003**, *36*, 6503−6510.
(31) Gil, E. S.; Hudson, S. M. *Prog. Polym. Sci.* **2004**, *29*, 1173−1222.
(32) Garret-Flaudy, F.; Freitag, R. *J. Polym. Sci., Part A: Polym. Chem.* **2000**, *38*, 4218−4229.
(33) Although the concentrations used here for turbidity measurement are about 30 times smaller than those used for temperature-dependent ^{1}H NMR measurements, they are still 30−200 times higher than their critical association concentrations, which were estimated by fluorescence spectroscopy to be around 6 and 50 mg·L^{-1} for **PLG$_{86}$PN$_{360}$** and **PLG$_{600}$PN$_{360}$** at pH 10.0.
(34) Aseyev, V.; Hietala, S.; Laukkanen, A.; Nuopponen, M.; Confortini, O.; Du Prez, F. E.; Tenhu, H. *Polymer* **2005**, *46*, 7118−7131.
(35) Lutz, J. F.; Weichenhan, K.; Akdemir, Ö.; Hoth, A. *Macromolecules* **2007**, *40*, 2503−2508.
(36) Cölfen, H.; Mann, S. *Angew. Chem., Int. Ed.* **2003**, *42*, 2350−2365.

BM700729T